Received: 28 January 2021 | Revised: 11 March 2021 | Accepted: 11 March 2021

DOI: 10.1002/pen.25691

RESEARCH ARTICLE

POLYMER ENGINEERING AND SCIENCE WILEY

In-situ investigation of dielectric properties and reaction kinetics of a glass-fiber-reinforced epoxy composite material using dielectric analysis

Shuang Yan[1] | **Harald Zeizinger**[1] | **Clemens Merten**[2] | **Siegfried Schmauder**[1]

[1]Institute for Materials Testing, Materials Science and Strength of Materials, University of Stuttgart, Stuttgart, Germany

[2]Institute of Chemical Process Engineering, University of Stuttgart, Stuttgart, Germany

Correspondence
Shuang Yan, Institute for Materials Testing, Materials Science and Strength of Materials, University of Stuttgart, Pfaffenwaldring 32, D-70569 Stuttgart, Germany.
Email: shuang.yan@imwf.uni-stuttgart.de and shuang.yan.st@gmail.com

Abstract

Monitoring the curing behavior of a thermosetting material is a key issue for ensuring a stable manufacturing process (e.g., injection molding). Dielectric analysis (DEA), which is applicable for online-monitoring, is used to investigate the curing behavior of a glass-fiber-reinforced epoxy molding compound. At first, the influences of experimental settings (pressure, temperature, and frequency) on dielectric responses (dielectric loss and ion viscosity) are characterized in a fully crosslinked material. Results show a significant impact of temperature and frequency on dielectric responses. Furthermore, DEA is combined with differential scanning calorimetry (DSC) to investigate dielectric properties depending on crosslink density under non-isothermal and isothermal conditions. The results show that DEA can detect cure changes only for a crosslink density <80%. Finally, reaction kinetics, which can predict the crosslink density, is derived using DSC and validated through DEA for determining the best suitable kinetic expression for the investigated material. The crosslink density, estimated by reaction kinetics, can be correlated with the dielectric properties.

KEYWORDS

cure behavior, DEA, dielectric properties, DSC, epoxy, reaction kinetics

1 | INTRODUCTION

Thermosets that are widely used in industry are reactive polymers. Non-cured thermoset material contains many monomers, which start to crosslink from a specific temperature during processing. Three-dimensional molecular structures built spatially throughout the crosslinking process give the hardened thermoset outstanding mechanical properties at high temperatures and good chemical resistance. It is essential to understand the changes in material behavior during processing, for example, in the injection molding process. The thermoset's hardening and the released large amount of reaction enthalpy, which cause changes in temperature and dynamical viscosity in the material, could lead to manufacturing and material faults.

There are several measuring methods for observing the curing progress of thermosets: differential scanning calorimetry (DSC), dielectric analysis (DEA), Raman spectroscopy, Fourier transform infrared spectroscopy (FTIR),[1–3] and ultrasonics.[4] Based on the amount of heat released from crosslinking reactions, DSC is a classical method to analyze the relationship among crosslink density, temperature, and time,[5–8] which is often expressed in an

empirical model termed reaction kinetics (Equation 5). However, DSC is only useful in the laboratory environment and requires sample preparation in advance. Instead, since DEA is non-destructive and can be used for in-situ monitoring, DEA can be applied in the engineering area to track changes in a material's cure. Applications of the DEA technique exist in the polymer field, such as for analyzing relaxation properties that depend on temperature and frequency[9–13] and for monitoring the curing process in a thermosetting material.[3,12–19] Changes in dielectric responses, such as dielectric conductivity, dielectric loss, and ion viscosity, are related to the material properties' changes during curing, like glass-transition temperature,[16,18] cure reaction onset, and cure end.[14] The application of DEA for online-monitoring was reported in the autoclave process[14] and during the pressing process.[15] A correlation was provided between ion viscosity at the end of production and the transverse tensile strength.[15] The conductivity rises if the Newtonian viscosity decreases before gelation. During curing, pure epoxy resin has a similar conductivity as resins with fiber contents between 20% and 40%.[19] Yuste-Sanchez et al.[3] have investigated the curing behavior at 80°C and the post-curing behavior at 140°C of a pure resin and composite using DEA combined with FTIR and Raman spectroscopy. Based on molecular changes, FTIR and Raman spectroscopy were used to determine the crosslink density, which was compared with the degree of crosslinking calculated according to DEA signal (permittivity and dielectric loss). An apparent deviation between the crosslink density values determined through DEA and spectroscopic methods could be identified, although curves of crosslink density derived through both methods have a similar shape. The start of curing in the material (crosslink density = 0%) was set as the time point when the target temperature (80°C) was reached, while the sample was already placed in the dielectric cell during heating the cell from room temperature to 80°C. In this experiment, some resin cure probably occurred and was not considered for the crosslink density calculation using the DEA signal. In addition, the effect of varied frequencies on dielectric responses was obtained in curing and post-curing.

Our work aims to provide a way to investigate the correlation between dielectric properties and the curing behavior of thermosetting composites (e.g., a glass-fiber-reinforced epoxy molding compound) in the manufacturing process, whose findings can be transferred from the laboratory into industrial application. Since experimental configurations and material properties affect dielectric responses, the first step was to characterize the influences of experiment settings (pressure, temperature, and frequency) on dielectric responses (dielectric loss and ion viscosity) in fully crosslinked materials. Experiments on fully cured materials enable better understanding of how curing influences the DEA signals. The next step was to analyze the dielectric properties in correlation with crosslink density using non-isothermal and isothermal DEA combined with DSC. In particular, to avoid pre-curing in the material during heating, uncured samples are placed into the measuring chamber only after the target temperature is reached. After the feasibility for monitoring the curing behavior via dielectric properties is provided, an approach is developed to use reaction kinetics to predict the crosslink density correlated with the dielectric properties as a function of processing temperature and time. Reaction kinetics in different expressions are derived using dynamic DSC and then are compared to the results of crosslink density in DEA samples tempered at different temperatures and durations. The best suitable reaction kinetic expression will be determined for the investigated glass-fiber-reinforced epoxy molding compound.

2 | EXPERIMENTAL PROCEDURE

2.1 | Material and sample preparation

A glass-fiber-reinforced epoxy molding compound (EP) used in this study was purchased from Raschig GmbH and stored at <15°C, in which the mass ratio of the polymer matrix (epoxy resin, hardener, and catalyst) and glass-fiber is 25:75. The material contains bisphenol A diglycidyl ether (DGEBA) epoxy resin base, and the curing agent is a modified amine type. The glass transition temperature (measured using 20°C/min in DSC) is about 48°C, and the density at room temperature is 1.9–2.0 g/cm^3.

Reproducible sample preparation for the DEA experiments is an essential prerequisite for reproducible experiments. Samples were 1.000 ± 0.025 g and prepared at room temperature with a compression force of 100 kN for 5 min. Samples had a cylindrical shape with a diameter of 13 mm and a thickness of 4 mm to ensure full coverage of the sensor surface (see Figure 1).

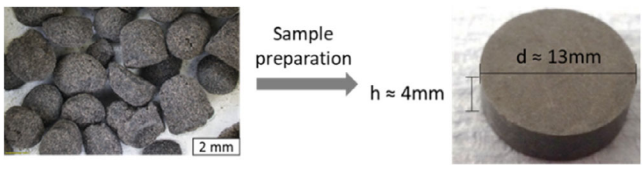

FIGURE 1 Sample preparation at room temperature from loose granules to a cylindrical specimen [Color figure can be viewed at wileyonlinelibrary.com]

2.2 | Differential scanning calorimetry

Differential scanning calorimetry (DSC Q100, TA Instruments–Waters LLC) measures a material's calorimetric changes. A small piece of material weighting 12 ± 2 mg was prepared directly into Tzero aluminum hermetic pans with a lid. The reaction kinetic is a temperature- and time-dependent empirical function determined by non-isothermal DSC performed at constant heating rates of 2, 5, 10, 15, and 20°C/min from 25 up to 250°C and with nitrogen N_2 as the purge gas.

2.3 | Dielectric analysis

Dielectric analysis (DEA) measures a material's response to an applied electric field. The electrical current I_{electr} flowing through a sample as a response to an alternating electric field is a function of the field frequency f and the applied electrical voltage U_{electr}. DEA analyzes the changes in the polymer's dielectric properties (e.g., dielectric loss, dielectric constant), which depend on the changes in molecular and morphological structures in the material.

A thermoset material is a dielectric material that stores energy and consumes energy in an electric field. A dielectric material has a capacitive and conductive character induced by the dipoles and ions that exist in the material. The dielectric responses in the material are caused by the dipole orientation and ion mobility. With no electric field, dipoles and ions orientate randomly. Under an electric field, the dipoles orientate and ion movement conducts electric current to the electrode with opposite polarity. Simultaneously, another effect caused by ion mobility toward the electrode is electrode polarization, meaning that the ions accumulate in a thin layer (charge layer) immediately beneath the polymer surface. According to the capacitive and conductive character in a dielectric material, the relative permittivity ε_r for the investigated material is written as a complex quantity (Equation 1).

$$\varepsilon_r(\omega) = \varepsilon'(\omega) - i \cdot \varepsilon''(\omega), \tag{1}$$

The real part ε' (dielectric constant) interprets the amount of stored electric energy (reversible) in the material, mainly associated with dipole orientation. In contrast, the imaginary part ε'' (dielectric loss) describes the loss of energy in a dielectric material influenced by both dipole relaxation and ion mobility.[20] A function of dielectric loss ε'', which considers both influences (dipole relaxation and ion mobility) independently, is expressed in Equation 2.[20,21]

$$\varepsilon'' = \underbrace{\frac{(\varepsilon_u + \varepsilon_{rl})\omega\tau}{1 + \omega^2 \cdot \tau^2}}_{\text{dipole relaxation}} + \underbrace{\frac{\sigma}{\omega\varepsilon_0}}_{\text{conductivity}}. \tag{2}$$

ε_u is unrelaxed permittivity, ε_{rl} is relaxed permittivity, τ is relaxation time, ε_0 is the vacuum permittivity, ω is angular frequency ($\omega = 2\pi f$), and σ is ionic conductivity. If the condition $\frac{(\varepsilon_u + \varepsilon_{rl})\omega\tau}{1 + \omega^2 \cdot \tau^2} \ll \frac{\sigma}{\omega\varepsilon_0}$ is satisfied, dipole relaxation in ε'' can be neglected. The ionic conductivity dominates ε'' at limiting low frequency so that the impact of dipole orientation is negligible.[20] In this case, the function of ε'' is written as follows (Equation 3).

$$\varepsilon'' = \frac{\sigma}{\omega\varepsilon_0}. \tag{3}$$

the ion viscosity η_{ion} is defined as the reciprocal value of ionic conductivity σ, shown in Equation 4, and can be used to monitor the curing process.[15,22]

$$\eta_{\text{ion}} = \frac{1}{\sigma}\eta_{\text{ion}} \approx \frac{1}{\omega\varepsilon_0\varepsilon''} \text{ (When dipole relaxation is negligible)}, \tag{4}$$

A dielectric analyzer (DEA 288 Ionic, NETZSCH-Gerätebau GmbH), consisting of the DEA electronics and a sensor TMC 18/3A HT, was used to study dielectric behavior. A lab press with an integrated DEA sensor (Paul-Otto Weber GmbH) can apply heat, pressure, and frequency to the material simultaneously (see Figure 2).

The initial step was to analyze the modified experimental setting's effects on dielectric properties to determine an optimal experimental configuration and ensure stable experimental reproducibility. This step used the fully crosslinked EP sample, and experimental configurations were set with varying clamping forces (6, 8, and 10 kN), a frequency sweep (1 Hz–10 kHz), and various temperatures (50, 100, 150, 200, 250, and 280 °C).

The next step was to investigate the dielectric properties in correlation with the material's curing behavior quantitatively. Since the curing reaction is time- and temperature-dependent, the samples were measured under different thermal conditions (isothermal and non-isothermal). The isothermal measurement means that the sample will be measured at a constant temperature T for a duration t. Under non-isothermal experimental conditions, the temperature will heat up with a constant heating rate β from T_1 to T_2.

DEA measurements were carried out with a frequency sweep (1 Hz–10 kHz) at a heating rate of 2°C/min, and DSC measured the crosslink density with

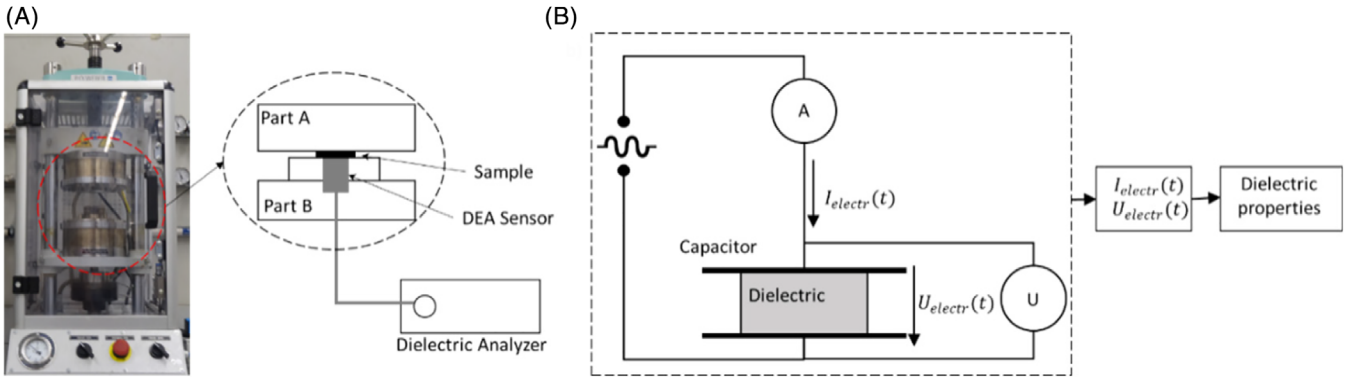

FIGURE 2 Dielectric analysis (DEA) lab press. (A) Configuration of the lab press consisting of DEA electronics, a sensor, a lower, and upper part heated with electric heating tapes controlled by a temperature sensor in each piece. (B) Schematic configuration of the DEA electronics and sensor. Dielectric properties, such as dielectric loss, dielectric constant, and loss factor, will be determined based on DEA outputs [Color figure can be viewed at wileyonlinelibrary.com]

the same heating rate. For estimating the changes in dielectric properties in correlation with crosslink density under isothermal conditions, experiments were operated at 125 and 135°C. While the investigated epoxy composite begins to cure in a temperature range between 90 and 120°C, the processing temperature, for example, in an injection molding process, is higher than 150°C, which means a high reaction speed and a short curing time. Regarding the material's temperature sensitivity, the two temperature levels (125 and 135°C) were chosen to ensure a sufficient curing time for removing the partially cured samples. The experimental operation of isothermal DEA measurements is described as follows. The EP sample was placed into the DEA chamber at target temperatures of 125 and 135°C, which took about 1 min. The clamping force was kept constant during the measuring. The materials, heated for 3, 6, 9, 11, and 31 min, respectively, were removed from the lab press and immediately cooled down to terminate the chemical reaction. And then, the proportion of crosslinking reactions α that has occurred during dielectric measurement (at temperature T for duration t) was determined by DSC. DEA-results measured under isothermal conditions were applied to validate the reaction kinetics determined with the DSC method.

3 | RESULTS AND DISCUSSION

3.1 | Influence of experimental setting on DEA response

In dependence on machine setting and material property, diverse factors could influence dielectric responses during dielectric measurement of a thermosetting material. The impacts caused by various parameters on the measuring signals were analyzed and are discussed separately in the following sections.

The first step was to investigate the change in dielectric responses caused by varying the machine parameters (pressure, temperature, frequency). Therefore, the fully crosslinked EP material was used in DEA experiments without considering the influence of chemical reactions on measuring results.

Figures 3(A), (B) show the results of dielectric loss ε'' and ion viscosity η_{ion} measured with varying clamping forces (6–10 kN) and a frequency sweep (1 Hz–10 kHz) at various temperatures (50–280°C). The scattering of dielectric loss ε'' and ion viscosity η_{ion} measured at different pressures is larger at low frequency (≤10 Hz) than at high frequency (>10 Hz). According to the results, the impact of the varied pressures on dielectric responses (dielectric loss and ion viscosity) is not to be identified. Since the TMC sensor is an interleaved capacitor, meaning that the penetration depth and the contract surface will be consistent under varied pressures. Therefore, in further experiments for analyzing the dielectric properties related to crosslinking behavior, the clamping force was kept constant.

In both subplots (A), (B) the dielectric loss increases, and the ion viscosity drops while the temperature rises from 50 to 280°C. Since the material is already completely cured, changes with increasing temperature are due exclusively to softening until decomposition occurs. Ion diffusion is enhanced with more thermal energy, which causes both higher ionic conductivity and more friction losses between the molecules. The growth of dielectric loss and the drop of ion viscosity with increasing temperature, caused by more ion movement at higher temperature, is smaller when measuring frequency increases. For example, listed in Table 1, the growth of dielectric loss $\Delta\varepsilon''$ (50–280°C) at 1 Hz is about 40,000, while the $\Delta\varepsilon''$

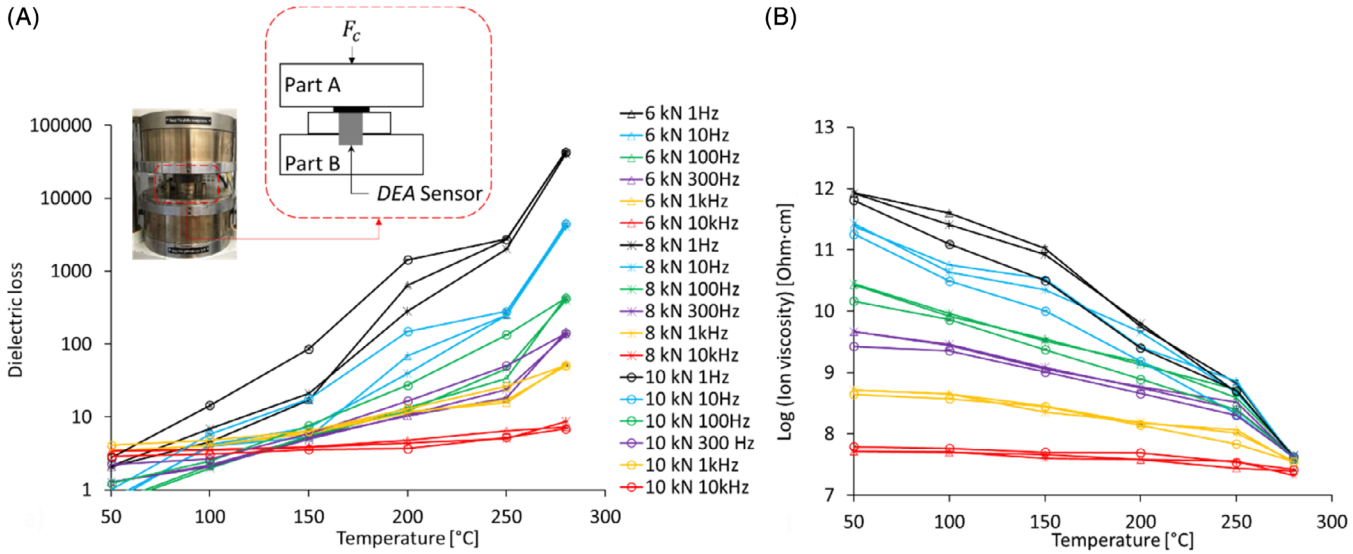

FIGURE 3 Results of dielectric loss ε'' (A) and ion viscosity η_{ion} (B) determined with clamping force *Fc* (6–10 kN) and frequency sweep (1 Hz–10 kHz) at various temperatures (50–280°C). Part A and B in the dielectric analysis (DEA) lab press were closed with a fully cured sample. Icons (pressure): Δ = 6 kN, x = 8 kN, o = 10 kN). Colors (frequency): Black = 1 Hz, blue = 10 Hz, green = 100 Hz, purple = 300 Hz, yellow = 1 kHz, red = 10 kHz [Color figure can be viewed at wileyonlinelibrary.com]

TABLE 1 Overview of absolute values and percentages of growth and drop in dielectric loss and ion viscosity, depending on experimental settings, shown as an example

Influence of temperature (50–280°C) at two frequencies (1 Hz and 10 kHz)					
	1 Hz		**10 kHz**		
$\Delta\varepsilon''$ [−]	+40,000 (+2·10^6%)		+4 (+100%)		
$\Delta\log(\eta_{ion})$ [Ohm·cm]	−4.5 (−45%)		−0.2 (−2.5%)		
Influence of frequency (1 Hz to 10 kHz) at 50, 100, 150, 200 and 280°C					
	50°C	**100°C**	**150°C**	**200°C**	**280°C**
$\Delta\log(\eta_{ion})$ [Ohm·cm]	−4.3 (−35%)	−3.7 (−32%)	−3.5 (−29.2%)	−2.0 (−21%)	−0.2 (−3.2%)

(50–280°C) at 10 kHz is four. Furthermore, the decrease of ion viscosity $\Delta\log(\eta_{ion})$ from 50 to 280°C at 1 Hz is equal to 4.5 Ohm cm, a 45% decreased value. The reduction $\Delta\log(\eta_{ion})$ from 50 to 280°C at 10 kHz is 0.2 Ohm cm, a 2.5% dropped amount. The results also show that ion viscosity difference from 1 Hz to 10 kHz decreased with increasing temperature, for example, $\Delta\log(\eta_{ion})$ is equal to 4.3 Ohm cm at 50°C, $\Delta\log(\eta_{ion})$ is 3.5 Ohm cm at 150°C, and $\Delta\log(\eta_{ion})$ is 2.0 Ohm cm at 200°C. Moreover, the ion viscosity value was 7.6 ± 0.1 Ohm cm at 280°C at all measured frequencies.

3.2 | DEA results under isothermal and non-isothermal condition

In this part, the changes in dielectric properties caused by the chemical process, whereas the reaction heat occurs and the material phase changes, were analyzed. Because the curing reaction is a time- and temperature-dependent procedure, the samples were measured under different thermal conditions (isothermal and non-isothermal).

DSC and DEA measurements were performed at a low heating rate of 2°C/min from 50 to 200°C to investigate dielectric behavior under non-isothermal conditions and the results were correlated with crosslink density. 2°C/min was chosen so that the lab press and the sample could heat up with a homogeneous temperature distribution. Non-isothermal DEA results (dielectric loss and ion viscosity) are plotted in Figure 4(A), (B). The peak height of dielectric loss decreases with increasing frequency while the dielectric loss value at 10 kHz is constant through the entire measurement, which indicates the disappearance of conductivity induced by ion mobility. Similarly, ion viscosity curves become flatter with increasing frequency until a straight line occurs at 10 kHz. The

movement of ions is blocked at the high frequency of 10 kHz, meaning that ions cannot reorient, accumulate, and build up the electrode layer during the short time at high frequency. Hence, no information about curing can be ascertained at a frequency ≥10 kHz.

Figure 5(C) shows the results of crosslink density $\alpha(T, t)$, dielectric loss $\varepsilon''(T, t)$, and ion viscosity $log(\eta_{ion})$ measured at 1 Hz, whereby the rate of ε'' (T, t) and the rate of $log(\eta_{ion})$ are shown in plots (A) and (B). At 50°C, the sample is an uncured solid and contains no free movable ions, which could conduct the electric current, and hence the measured dielectric loss is approximately zero. The molecules begin to ionize, for example, become positively or negatively charged, with rising temperature, which is attributed to the reactive amine groups in the hardener becoming deprotonated. The material transitions from a solid to a highly viscous liquid, meaning that ion movement got more active in a lower viscosity material. The ion conductivity raised, and the electrode polarization decreased until 108°C, associated with higher dielectric loss and lower ion viscosity. Since the epoxy group structure is not hydrogen saturated, it will be protonated into the hydroxyl group during the crosslinking reaction. According to DSC results, the material started crosslinking at 90°C (point g) and achieved a crosslink density of <10% at 108°C (point h), where the maximal dielectric loss and the minimal ion viscosity occurred. The liquification and crosslinking process in the material overlapped in the temperature range (point g–h), but liquification dominated, which caused a continuous decrease of ion viscosity until it reached the minimum value at point h. Since the ion viscosity correlates with dynamic viscosity, the hardening in the material increased from the turning point h rapidly, meaning that the curing process was accelerated and the material changed from liquid to solid (point j). Hardening means that epoxy base resins crosslinked with hardeners and built up the macromolecules connected to changes in the material's molecular structures. As the molecules increase in molecular weight, they restricted ion movement more strongly so that the dielectric loss near point j was smaller. From point j, where the crosslink density is equal to 80%, two effects overlapped in the solid material: further curing and softening caused by increasing temperature. Further curing contributed to the hardening of the material, and increasing temperature led to the material's softening. A slightly arising dielectric loss obtained in Figure 5 indicates that softening dominates and the remaining ion movement is more active.

According to the results measured by 100 Hz shown in Figure 6(B), the value of dielectric loss reduces from the peak height of 25 and plateaus from 135°C, while ion

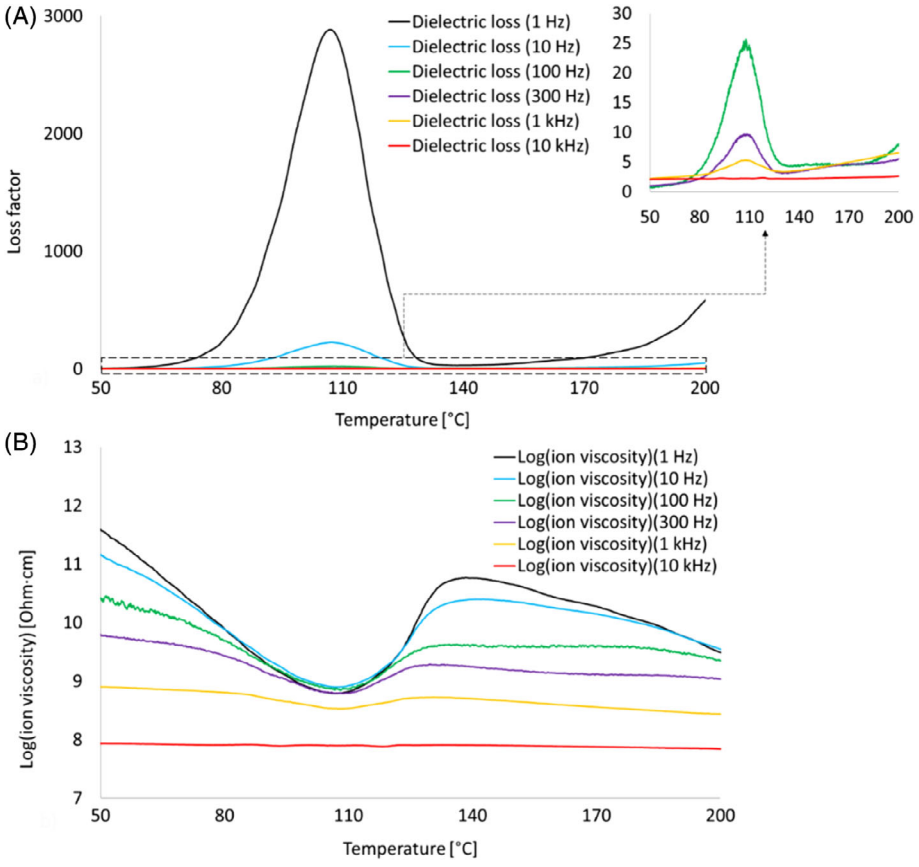

FIGURE 4 Dielectric loss (A) and ion viscosity (B) measured at a heating rate of 2°C/min with frequencies of 1 Hz–10 kHz [Color figure can be viewed at wileyonlinelibrary.com]

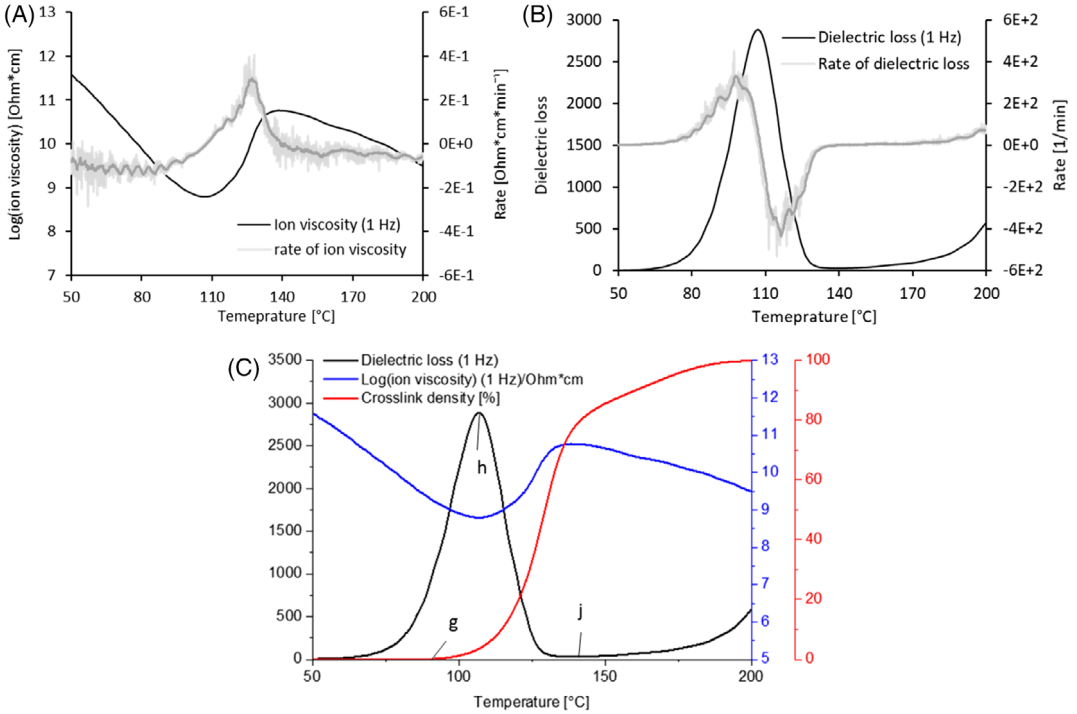

FIGURE 5 Overlapped results of differential scanning calorimetry (DSC) and dielectric analysis (DEA) at a frequency of 1 Hz. (A) Rate of ion viscosity. (B) Rate of dielectric loss. (C) Curves of dielectric loss, ion viscosity, and crosslink density [Color figure can be viewed at wileyonlinelibrary.com]

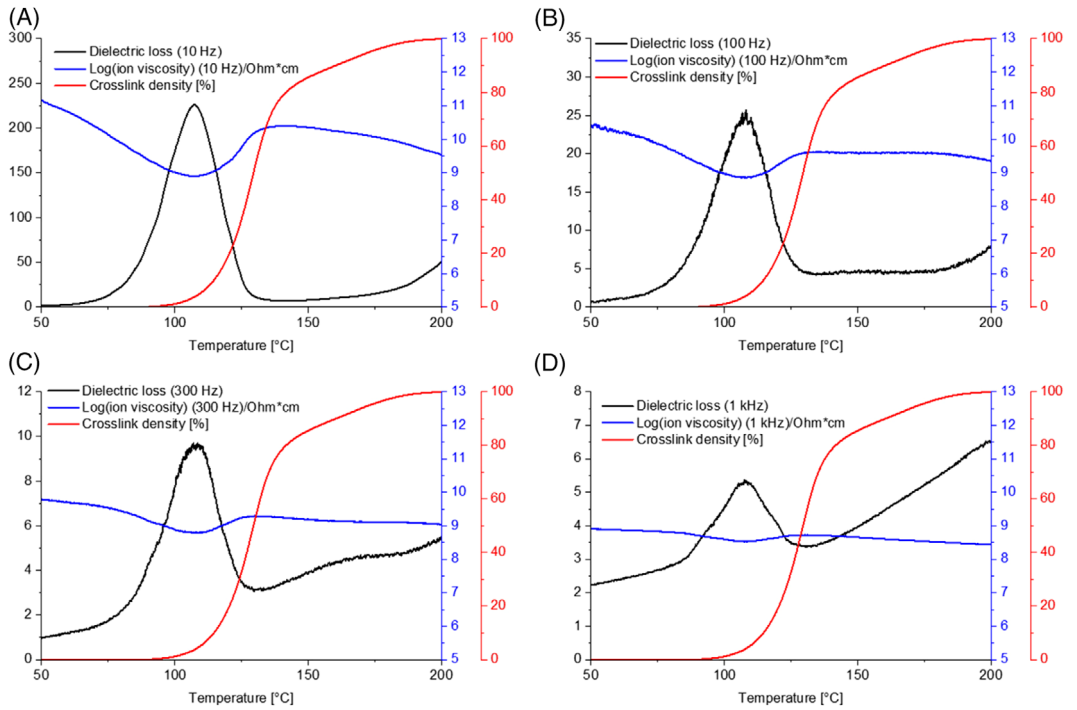

FIGURE 6 Overlapped results of dielectric analysis (DEA) and differential scanning calorimetry (DSC) at a frequency of 10, 100, 300 Hz, and 1 kHz, respectively, in (A)–(D) [Color figure can be viewed at wileyonlinelibrary.com]

viscosity drops very slowly. Simultaneously, the crosslink density is equal to 50%, meaning that curing was still occurring. The curing process finished at a temperature of ~185°C, indicating that the sample was fully crosslinked. Above 185°C, the ion viscosity reduced while the dielectric loss increased because the diffusion of the remaining ions through the tight molecular structure was encouraged by more thermal energy. In previous studies, the minimal ion viscosity defined as the beginning of crosslinking ($\alpha = 0\%$) corresponds to the maximal dielectric loss.[14–16] In our material, which has a phase change (solid–liquid–solid), crosslinking begins in the liquid phase, meaning that the material generally has a small early curing extent at the minimal ion viscosity and maximal dielectric loss. Furthermore, DEA could monitor most of the curing process. However, in this material DEA cannot monitor curing above a crosslink density of 80%. The material gets highly viscous or even hard at a high crosslink amount (>80%) and contains a low ion concentration, decreasing continuously due to further curing. Simultaneously, the crosslinked macromolecular structures become close-meshed and restrict the ion movement very strongly, which causes a lower ion conductivity. Electrode polarization caused by the remaining ions that accumulate in the electrode-polymer-surface also becomes very slight. Therefore, all effects lead to low dielectric responses measured by DEA, and hence is not sensitive enough for tracking the crosslinking process. In addition, based on the results shown in Figure 6(A), (B), at a frequency of ≤100 Hz, DEA could not detect the thermal effect (e.g., dielectric loss curve shifts to a higher value) caused by increasing temperature. Furthermore, at a high frequency of ≥1 kHz (Figure 6(D)), the dielectric response gets too slight. Therefore, for the following measurements, the measuring frequency was set as 300 Hz.

For DEA measurements performed under isothermal conditions, the EP-samples were measured at a constant temperature from an uncured state to a fully cured state for obtaining the dielectric responses. The heating chamber was opened after reaching the target temperature to insert the sample carrier so as to prevent curing during heat up, however, this step has high heat loss, and the desired ambient temperature cannot be maintained. This problem is worse for DSC than DEA. Since the DSC method is not accurate for isothermal measurement, a novel approach was applied in this study to find the correlation between the dielectric properties and crosslink density. DSC measured EP-samples tempered in a DEA lab press for 3, 6, 9, 11, and 31 min at 125 and 135°C that are shown in Figures 7(A) and (C) to estimate the crosslink density. Figure 7(B) shows dielectric loss change depending on the crosslink density in the investigated material. The dielectric loss decreased nonlinearly in the time range from 3 to 31 min at a constant temperature. After the crosslink density was about 80%, the drop of dielectric loss slowed down and tended to plateau, while the subsequent reaction was still in progress. This case is similar to non-isothermal DEA measurement in that the curing process can hardly be detected after the investigated material gets a crosslink density above 80%. In the pure resin containing no glass fibers, the reaction partners' mobility related to ion movement in DEA is higher than in the epoxy/glass fibers composite. In pure resin with the same crosslink density, stronger measured dielectric responses can be expected vs. the epoxy composite. The dielectric loss will still have a non-linear correlation to curing progress in pure resin since the loss is determined by the curing mechanism and should, therefore, not be affected by glass fibers that are not involved in the curing reaction. However, the dielectric loss curve depending on crosslink density in pure resin could shift to higher values with a similar curve shape. In addition, the crosslink densities estimated at 125 and 135°C in this step were applied to validate the reaction kinetics, and the results will be discussed in the following section.

3.3 | Reaction kinetics

Reaction kinetics describes the rate of chemical reaction, usually shown in Equation 5,[23–25] which considers temperature-, pressure- and concentration-dependency $k(T)$, $h(p)$, and $f(\alpha)$.

$$d\alpha/dt = k(T)\cdot f(\alpha)\cdot h(p), \tag{5}$$

since pressure p was kept constant during the chemical reaction, the pressure-dependency can be ignored. The temperature-dependency is usually expressed as $k(T) = A\cdot\exp((-E_a)/(R_{gas}\cdot T))$, generally known as the Arrhenius equation, consists of the material-related activation energy E_a and pre-exponential term A. R_{gas} is the gas constant (= 8.314 J/[mol·K]). Equation 5 can be rewritten as Equation 6.

$$d\alpha/dt = A\cdot\exp\left(\left(-E_a\right)/\left(R_{gas}\cdot T\right)\right)\cdot f(\alpha). \tag{6}$$

Since epoxy resins react with hardeners exothermic, the temperature- and time-dependent crosslink density can be calculated according to the ratio of released heat quantity $H_{release}$ to the maximum heat quantity H_{max} in a fully cured state (Equation 7). For determining the maximum reaction heat H_{max}, the non-cured material, immediately after material delivery, was measured using the DSC method until no more released reaction heat was

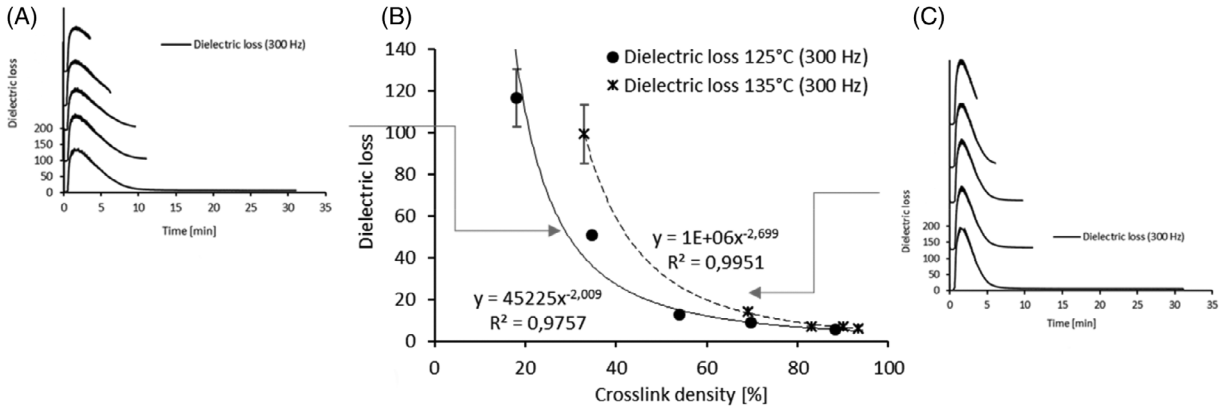

FIGURE 7 Dielectric loss at 125 and 135°C. (A) Curves of dielectric loss measured with 300 Hz at 125°C. (B) Correlation between dielectric loss and crosslink density measured with 300 Hz at 125 and 135°C. (C) Curves of dielectric loss measured with 300 Hz at 135°C. Differential scanning calorimetry (DSC) measured the samples heated in the lab press for a heating duration of 3, 6, 9, 11, and 31 min, respectively, to determine the crosslink density

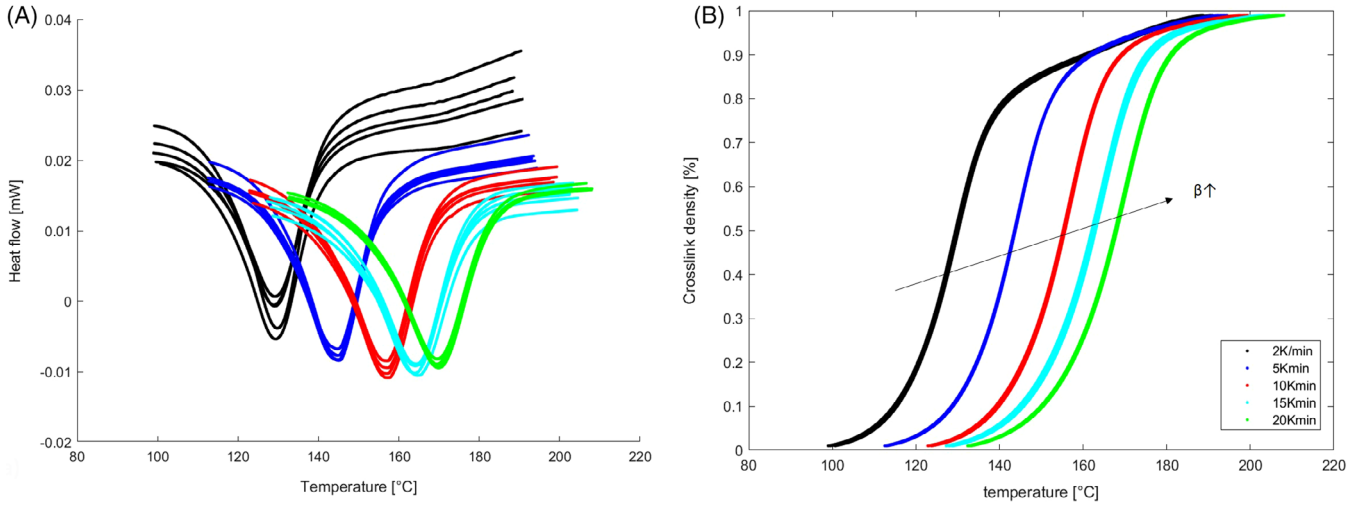

FIGURE 8 Heat flow (A) during the cure reaction and the resulting crosslink density (B) determined by DSC with different heating rates (2, 5, 10, 15, and 20°C/min) [Color figure can be viewed at wileyonlinelibrary.com]

obtained. The average of the total reaction heat calculated from repetitive DSC measurements is $H_{\max} = 51.77$ J/g. The crosslink density ranges from 0 (non-cured) to 1 (fully cured).

$$\alpha_{T,t} = H_{\text{release}}/H_{\max}. \tag{7}$$

Figure 8 shows the DSC curves measured at heating rates from 2 to 20°C/min in subplot (A), and the resultant crosslink density determined using a linear baseline in (B). The peak-temperature, where the maximum reaction rate occurs, increases with increasing heating rate, which agrees with previous studies.[17,26] In addition, the curves of crosslink density shift with increasing heating rate to a higher temperature, provided in earlier reports.[17,26] Figure 9 shows the Kissinger plot $\ln(\beta/T_p^2)$ versus $1/T_p$ according to the Kissinger-method,[27] which is suitable for a one-step cure reaction, and the activation energy E_a for the investigated material is estimated as 77.27 kJ/mol.

The reaction model $f(\alpha)$ is an empirical equation with different expressions, such as *nth*-order, *nth*-order catalytic, Prout–Tompkins, and Sestak–Berggren reaction model. The reaction models were fitted with the Levenberg–Marquardt algorithm (with a confidence interval of 95%) to the data $d\alpha/dt$ versus α, and the results for the fitting constants are listed in Table 2. The reaction kinetics (Equation 6) with different kinetic models $f(\alpha)$ (listed in Table 2) were solved at two temperatures (125 and 135°C) by temporal integration in Matlab.

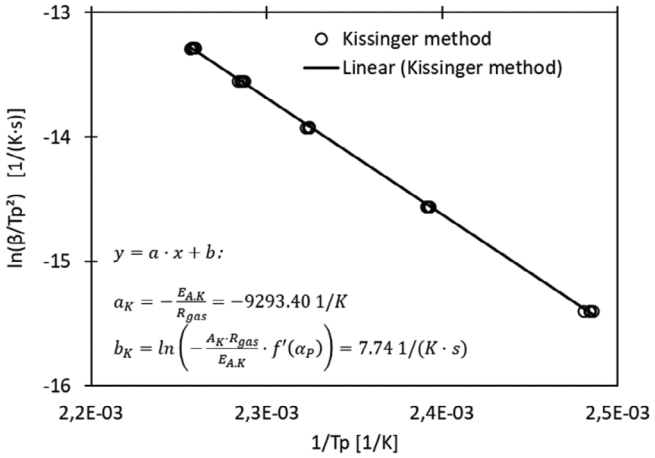

FIGURE 9 Determination of parameters a_k and b_k in the linear function according to the Kissinger method, including the activation energy E_a, pre-exponential term A and reaction model $f(\alpha)$

In Figure 10, the numerically calculated crosslink amounts are compared with experimental results measured in DEA samples heated at 125 and 135 °C for a heating duration from 3 to 31 min. The reaction kinetics with the *nth*-order reaction model provides the best match with experimental results and shows good agreement until achieving the crosslink amount of 90%, and the maximal crosslink density is reached earlier according to integrated reaction kinetics than in the experiment. In a real thermosetting material, the fully cured state is rarely achieved because some reactive groups cannot find a reaction partner. Indeed, the potential sources of error should be considered: selecting the baseline for calculating the reaction heat, analytical error in reaction kinetics derived by DSC measurements, sample geometry in DSC measurement causing non-homogenous heat transfer.

TABLE 2 Parameters in the reaction model estimated by regression of non-isothermal DSC measurements with a confidence interval of 95%

Reaction model	Expression $f(\alpha)$	Parameters
nth-order (*nO*)	$f(\alpha) = c_\alpha \cdot (1-\alpha)^{n_\alpha}$	$c_\alpha = 0.43$ and $n_\alpha = 0.27$, $\log A = 7.53$ 1/s, $R^2 = 0.90$
nth-order catalytic (*nOk*)	$f(\alpha) = c_\alpha \cdot (1-\alpha)^{n_\alpha} \cdot (1 + K_\alpha \cdot \alpha)$	$c_\alpha = 0.003$, $n_\alpha = 1.25$ and $K_a = 1296$, $\log A = 7.44$ 1/s, $R^2 = 0.99$
Prout–Tompkins (PT)	$f(\alpha) = c_\alpha \cdot \alpha^{m_\alpha} \cdot (1-\alpha)^{n_\alpha}$	$c_\alpha = 7.93$, $n_\alpha = 1.63$ and $m_a = 1.43$, $\log A = 7.34$ 1/s, $R^2 = 0.93$
Expanded Sestak–Berggren (SB1)	$f(\alpha) = c_\alpha \cdot \alpha^{m_\alpha} \cdot (1-\alpha)^{n_\alpha} \cdot [-\ln(1-\alpha)]^{p_\alpha}$	$c_\alpha = 3.12$, $n_\alpha = 6.12$, $m_a = -10.54$, and $p_a = 11.58$, $\log A = 7.55$ 1/s, $R^2 = 0.93$

Abbreviation: DSC, differential scanning calorimetry.

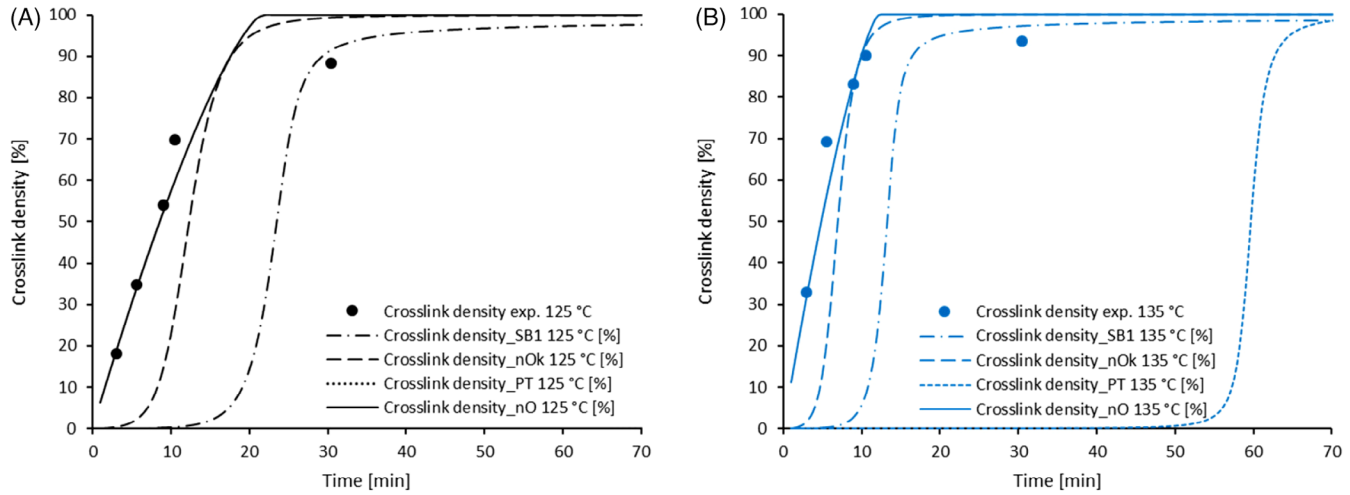

FIGURE 10 Comparison between numerical and experimental results of crosslink density at 125 and 135°C [Color figure can be viewed at wileyonlinelibrary.com]

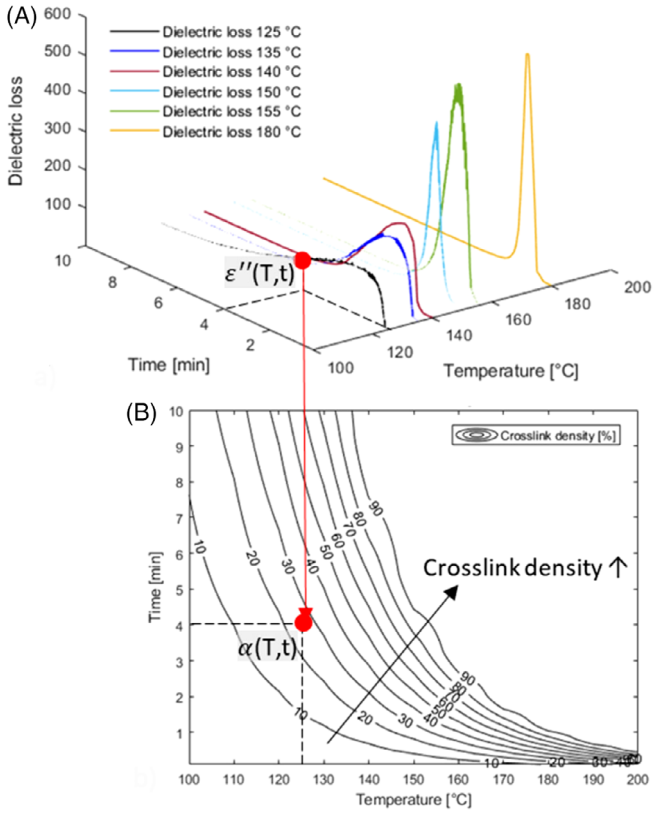

FIGURE 11 Dielectric loss $\varepsilon''(T,t)$ at 300 Hz depends on crosslink density $\alpha(T,t)$. (A) Curves of dielectric loss at temperatures of 125, 135, 140, 150, 155, and 180°C, respectively. (B) Contour plot of crosslink density distribution depending on temperature and time [Color figure can be viewed at wileyonlinelibrary.com]

After the best matching reaction model is determined, the correlation of the dielectric property (e.g., dielectric loss and ion viscosity) measured by isothermal DEA with the crosslink density determined by the reaction kinetics was estimated. Further isothermal dielectric measurements were performed at various temperatures. As an example, Figure 11(A) shows the evolution of dielectric loss $\varepsilon''(T,t)$ at different temperatures of 125, 135, 140, 150, 155, and 180°C with a constant frequency of 300 Hz. The dielectric loss increased at first after the sample was placed in the oven and heated up. After reaching the dielectric loss maximum, the loss began to decrease because of the accelerated curing process. The peak height of dielectric loss increases at higher isothermal curing temperature due to more ion movement at higher temperature, which causes more friction loss. The growth of dielectric loss peak from 125 to 140°C is equal to 80 while the increase from 140 to 150°C is 300. The rapid growth of dielectric between 140 and 150°C is caused by the catalyst activated at ≥150°C that accelerates the curing. Figure 11(B) shows the contour plot of crosslink density $\alpha(T,t)$ calculated based on Equation 6 with kinetic model *nth*-order (*nO*) (listed in Table 2), which has the best match to the isothermal DEA measuring results (shown in Figure 10).

4 | CONCLUSION

DEA was applied to investigate dielectric property changes (dielectric loss and ion viscosity) and correlated with cure behavior. Curing causes changes in temperature and dynamic viscosity in the material. Experimental settings and material properties affect the dielectric responses during the measurement. At first, the influences of experimental parameters (pressure, temperature, and frequency) on dielectric responses were investigated in the fully crosslinked material. No effect of applied pressure (6–10 kN) on dielectric responses was found. Increasing temperature (50–280°C) causes an increase in dielectric loss and a decrease in ion viscosity while increasing frequency (1 Hz–10 kHz) causes a decrease of dielectric loss and ion viscosity.

In the next step, the dielectric properties in correlation with crosslink density were investigated using non-isothermal and isothermal DEA combined with DSC. According to the non-isothermal DEA and DSC results, the liquification and curing phase overlapped and led to a small early curing extent when achieving maximal dielectric loss and minimal ion viscosity. Results show that dielectric analyses could detect most of the curing process (crosslink density of <80%). In the investigations of dielectric properties under isothermal conditions, the decrease of the dielectric loss has a nonlinear relationship with increasing crosslink density. Similar to non-isothermal DEA results, further curing progress cannot be detected in isothermal measuring from a crosslink density of 80% while the dielectric loss reaches a plateau.

Reaction kinetics, which can be determined by DSC, is applicable for predicting the crosslink density. The investigated material's activation energy was calculated using the Kissinger method and the regression method determined the parameters in different reaction model expressions. Since temporal integrations of reaction kinetics $d\alpha/dt$ with varying reaction models $f(\alpha)$ show a difference in crosslink density, the results were compared and validated using DEA data, and the best suitable reaction kinetic expression was determined for this investigated glass-fiber-reinforced epoxy molding compound. This resultant reaction kinetics was applicable for deriving the distribution of dielectric loss $\varepsilon''(T,t,f)$ corresponding to crosslink density $\alpha(T,t)$, which contributes to predict and monitor the cure behavior via the DEA technique. The derived reaction kinetic equation is

applicable in a numerical simulation, such as an injection molding process for a thermosetting material, where the reaction kinetics will be needed for computing the curing process.

ACKNOWLEDGMENTS

The authors would like to thank the company Mercedes-Benz AG for the financial support of this research. Open access funding enabled and organized by Projekt DEAL.

CONFLICT OF INTEREST

The authors declare that they have no known competing financial interests or personal relationships that could have appeared to influence the work reported in this paper.

ORCID

Shuang Yan https://orcid.org/0000-0002-7869-8934

REFERENCES

[1] R. Unger, U. Braun, J. Fankhänel, B. Daum, B. Arash, R. Rolfes, *Comput. Mater. Sci.* **2019**, *161*, 223. https://doi.org/10.1016/j.commatsci.2019.01.054.

[2] C. Ramírez, M. Rico, A. Torres, L. Barral, J. López, B. Montero, *Eur. Polym. J.* **2008**, *44*, 3035. https://doi.org/10.1016/j.eurpolymj.2008.07.024.

[3] V. Yuste-Sánchez, M. Hernández Santana, T. A. Ezquerra, R. Verdejo, M. A. López-Manchado, *Polym. Test.* **2019**, *80*, 106114. https://doi.org/10.1016/j.polymertesting.2019.106114.

[4] C. Gauthier, J. Galy, M. Ech-Cherif El-Kettani, D. Leduc, J.-L. Izbicki, *Int. J. Adhes. Adhes.* **2018**, *80*, 1. https://doi.org/10.1016/j.ijadhadh.2017.09.008.

[5] F. Mustata, N. Tudorachi, I. Bicu, *Compos., Part B* **2013**, *55*, 470. https://doi.org/10.1016/j.compositesb.2013.07.023.

[6] L. Granado, S. Kempa, S. Bremmert, L. J. Gregoriades, F. Brüning, E. Anglaret, N. Fréty, *J. Microelectron. Electron. Packag.* **2017**, *14*, 45. https://doi.org/10.4071/imaps.359903.

[7] M. Jouyandeh, S. M. R. Paran, S. S. M. Khadem, M. R. Ganjali, V. Akbari, H. Vahabi, M. R. Saeb, *Prog. Org. Coat.* **2020**, *140*, 105505. https://doi.org/10.1016/j.porgcoat.2019.105505.

[8] V. M. González-Romero, N. Casillas, *Polym. Eng. Sci.* **1989**, *29*, 295. https://doi.org/10.1002/pen.760290506.

[9] J. D. Badia, P. Reig-Rodrigo, R. Teruel-Juanes, T. Kittikorn, E. Strömberg, M. Ek, S. Karlsson, A. Ribes-Greus, *Compos. Sci. Technol.* **2017**, *149*, 1. https://doi.org/10.1016/j.compscitech.2017.05.026.

[10] A. M. Salaberría, R. Teruel-Juanes, J. D. Badia, S. C. M. Fernandes, V. Sáenz de Juano-Arbona, J. Labidi, A. Ribes-Greus, *Compos. Sci. Technol.* **2018**, *167*, 323. https://doi.org/10.1016/j.compscitech.2018.08.019.

[11] A. Martínez-Felipe, L. Santonja-Blasco, J. D. Badia, C. T. Imrie, A. Ribes-Greus, *Ind. Eng. Chem. Res.* **2013**, *52*, 8722. https://doi.org/10.1021/ie3031339.

[12] N. Luiz Dias Filho, H. Adolfo de Aquino, D. Souza Pereira, A. H. Rosa, *J. Appl. Polym. Sci.* **2007**, *106*, 205. https://doi.org/10.1002/app.26393.

[13] J. D. Badia, R. Teruel-Juanes, C. Acebo, O. Gil-Castell, A. Serra, A. Ribes-Greus, *Eur. Polym. J.* **2019**, *113*, 98. https://doi.org/10.1016/j.eurpolymj.2019.01.001.

[14] D. G. Lee, H. G. Kim, *J. Compos. Mater.* **2004**, *38*, 977. https://doi.org/10.1177/0021998304040563.

[15] U. Müller, C. Pretschuh, R. Mitter, S. Knappe, *Int. J. Adhes. Adhes.* **2017**, *73*, 45. https://doi.org/10.1016/j.ijadhadh.2016.07.016.

[16] H. Park, *J. Appl. Polym. Sci.* **2017**, *134*, 55. https://doi.org/10.1002/app.44707.

[17] M. Demleitner, S. A. Sanchez-Vazquez, D. Raps, G. Bakis, T. Pflock, A. Chaloupka, S. Schmölzer, V. Altstädt, *Polym. Compos.* **2019**, *40*, 4500. https://doi.org/10.1002/pc.25306.

[18] J. Chen, M. Hojjati, *Polym. Eng. Sci.* **2007**, *47*, 150. https://doi.org/10.1002/pen.20687.

[19] K. Nixdorf, G. Busse, *Compos. Sci. Technol.* **2001**, *61*, 889. https://doi.org/10.1016/S0266-3538(00)00174-3.

[20] J. Mijović, J. Kenny, A. Maffezzoli, A. Trivisano, F. Bellucci, L. Nicolais, *Compos. Sci. Technol.* **1993**, *49*, 277. https://doi.org/10.1016/0266-3538(93)90109-T.

[21] R. Raja Pandiyan, S. Chakraborty, G. Kundu, S. Neogi, *J. Appl. Polym. Sci.* **2009**, *114*, 2415. https://doi.org/10.1002/app.30720.

[22] J. Steinhaus, B. Hausnerova, B. Moeginger, M. Harrach, D. Guenther, F. Moegele, *Polym. Eng. Sci.* **2015**, *55*, 1485. https://doi.org/10.1002/pen.24100.

[23] M. R. Keenan, *J. Appl. Polym. Sci.* **1987**, *33*, 1725. https://doi.org/10.1002/app.1987.070330525.

[24] S. Vyazovkin, A. K. Burnham, J. M. Criado, L. A. Pérez-Maqueda, C. Popescu, N. Sbirrazzuoli, *Thermochim. Acta* **2011**, *520*, 1. https://doi.org/10.1016/j.tca.2011.03.034.

[25] M. Karcher, A. Chaloupka, F. Henning, S. Schmölzer, E. Moukhina, *Zeitschrift Kunststofftechnik* **2016**, *12*, 80.

[26] R. Hardis, J. L. P. Jessop, F. E. Peters, M. R. Kessler, *Compos. Part A: Appl. Sci. Manuf.* **2013**, *49*, 100. https://doi.org/10.1016/j.compositesa.2013.01.021.

[27] H. E. Kissinger, *Anal. Chem.* **1957**, *29*, 1702.

How to cite this article: Yan S, Zeizinger H, Merten C, Schmauder S. In-situ investigation of dielectric properties and reaction kinetics of a glass-fiber-reinforced epoxy composite material using dielectric analysis. *Polym Eng Sci*. 2021;1–12. https://doi.org/10.1002/pen.25691